European Journal of Geography

The publication of the European Journal of Geography (EJG) is based on the European Association of Geographers' goal to make European Geography a worldwide reference and standard. Thus, the scope of the EJG is to publish original and innovative papers that will substantially improve, in a theoretical, conceptual, or empirical way the quality of research, learning, teaching, and applying geography, as well as in promoting the significance of geography as a discipline. Submissions are encouraged to have a European dimension. The European Journal of Geography is a peer-reviewed open access journal and is published quarterly.

Received: 17/07/2026
Revised: 16/09/2026
Revised: 06/11/2026
Accepted: 08/11/2026
Published: 21/11/2026

Editor:
Dr Alexandros Bartzokas-Tsiompras

Research Article

Testing the Burn-to-Build Hypothesis for Greek Wind Energy: Multi-Scale Evidence from Fire Perimeters, Ignition Points, and Licensing Dates

Stavros Stromatas [1]✉

[1] Independent Researcher, Greece

✉ Correspondence: sstromts@gmail.com

Abstract: A recurring claim in Greece holds that wildfires are set deliberately to clear land for wind development. We test whether the national wind fleet shows the spatial and temporal signature such a mechanism would produce; intent is not observable from siting data. Using 2,958 turbines at 398 licensed stations and 1,644 EFFIS fire perimeters (2010 to 2024), we combine a use-availability case-control design on a wind-viable universe, an ignition-point analysis (FIRMS), and survival models dated at the installation licence. At the licence level, wind farms are modestly more likely than comparable wind-viable land to lie near burnt extent (fuel-adjusted odds ratio 1.34), but the association is absent at the turbine and physical-cluster units, loses significance when a licence is represented by one of its own turbines, and sits at the edge of the null under permutation inference. The point scale is null, we find no evidence that turbines are closer to fire ignition points than expected, installations do not follow prior fires once the event is dated at the installation licence, and larger farms are not more burnt-adjacent. One weak signal runs the other way: farms with a catchment fire in the three years after the production licence exceed expectation by 44 to 73%, not significantly. We read the residual as shared occupancy of dry, exposed uplands by wind resource and fire, an interpretation, not a tested result. The fleet shows no signature of systematic burn-to-build; this neither establishes nor excludes burnt-land siting of any single project.

Keywords: wind energy; wildfire; land use; use-availability; survival analysis; Greece

Highlights:

- There is no evidence that Greek wind turbines are preferentially sited on burnt land at the point, turbine or physical-development scale, or near estimated fire ignition points at any unit.
- A landscape-scale association appears at the licence unit but not at the turbine or physical-cluster unit, a dependence on the spatial unit (the modifiable areal unit problem).
- At the fleet level there is no spatial or temporal signature of systematic burn-to-build; individual cases lie outside the scope of this population-level test.

DOI: 10.48088/ejg.s.str.17.1.399.424
ISSN: 1792-1341
E-ISSN: 2410-7433

Copyright: © 2026 *by the authors. Licensee European Association of Geographers (EUROGEO). This article is an open access article distributed under the terms and conditions of the Creative Commons Attribution (CC BY) license.*

1. Introduction

The rapid expansion of onshore wind energy across fire-prone Mediterranean landscapes has been accompanied, in Greece, by a persistent public claim: that wildfires are deliberately set to clear forest which would otherwise block development, so that wind turbines are subsequently installed on the burnt land. The claim recurs in Greek media and social media and in local opposition to specific projects (Efstathiou, 2025; Panizio & Canetta, 2024). The related concern that licences are granted on burnt land has been put to Parliament (Manousos, 2024). The belief is also widely held: in a national survey of 2,005 respondents aged 17 and over in 2022, 55.1% agreed that wind turbines spring up after catastrophic forest fires and 73.4% that most fires are deliberately set (Metron Analysis, 2022). The question matters

beyond Greece, because similar suspicions attach to renewable-energy siting in many fire-prone regions. If the claim were true, it would imply that turbine locations coincide with previously burnt ground at a rate above what siting on wind grounds alone would produce, and that fire tends to precede installation in a way consistent with intent.

Testing such a claim rigorously is harder than it first appears, and the intuitive tests mislead in two distinct ways. First, turbines occupy very little ground, so any statistic of the form "turbine footprint as a fraction of burnt area" is tiny by construction and says nothing about preference; a vanishing ratio is fully compatible with strong selection, and a large ratio would be impossible regardless of behaviour. Second, and more fundamentally, the relevant comparison is not against all land or all burnt area but against comparable wind-viable land. Greece burns extensively every year, and wind development concentrates on exposed ridgelines that are themselves dry and fire-prone, so a raw overlap between turbines and burnt areas is expected even under siting entirely random with respect to burn history. Establishing preference requires a base rate defined on the land where turbines could plausibly be placed, and establishing the causal direction implied by the claim requires ordering fire against installation in time.

Whether a set of chosen locations is drawn preferentially from an available landscape is the use-availability problem of resource-selection analysis, set out in Section 2.3, in which "used" points are contrasted with a random sample of "available" background under covariate adjustment. Framing that contrast as cases against controls sampled from an eligible universe is the logic of spatial epidemiology (Elliott & Wartenberg, 2004). Separating genuine siting preference from landscape confounding, finally, is a recurring difficulty in studies of where energy and other infrastructure is built (Diffendorfer & Compton, 2014). The methods deployed here are therefore not specific to Greece; they transfer to any contested siting claim for which a defensible set of available locations and a credible time ordering can be constructed.

Prior analysis of Greek wind siting is dominated by work from the national industry association. Its peer-reviewed contribution (Vlamakis et al., 2026) quantifies land take rather than any relationship with fire; the specific claim tested here has been addressed only in a conference poster (Vlamakis et al., 2025) and an associated quantitative report (Hellenic Wind Energy Association, 2025). That work reports that wind farms occupy at most 0.07% of legally reforestable land, and that turbines installed after a fire cover 0.03% of the area burnt over the period 2008 to 2024, and it concludes that there is no correlation. Those figures are footprint-over-area ratios, small by construction, computed over reforestable or burnt land rather than over wind-viable land, and they carry no inferential test of preference or of time ordering. They can motivate the question but cannot resolve it.

This paper asks whether the national fleet displays the spatial and temporal signature that a systematic burn-to-build mechanism would produce. Because the answer depends on how a wind development is delimited, the tests are run at several units of analysis, administrative and physical, and we examine whether adjacent licences within one physical development belong to the same developer, which determines how that dependence should be read (Section 6.1). The paper's contribution is thus twofold: a substantive, evidence-based answer to a charged public question about Greek wind energy, and a methodological demonstration of how much the answer can depend on the unit of analysis, the spatial scale, the completeness of the landscape controls, and in particular on whether the unit is physical or administrative.

The analysis is organised around three questions, each matched to one test. The first asks whether fires tend to precede wind-farm installation in the catchments of existing stations, and what that raw ordering can and cannot show without a base rate (Test A, descriptive). The second asks whether wind farms are associated with burnt land more strongly than comparable wind-viable land would predict, once landscape confounders and the unit of analysis are accounted for (Test B, use-availability case-control). The third asks whether a prior fire raises the subsequent probability that eligible land receives an installation licence, so that any association is time-ordered in the direction the claim requires (Test C, time-varying survival). The objectives are to answer each question at several spatial scales and units, to separate landscape fire-proneness from any preference for burnt ground, and to state what a population-level pattern can and cannot say about individual projects.

2. Background and related work

Onshore wind siting is driven primarily by wind resource, terrain and access. Empirical, infrastructure-based studies of wind land take consistently find that the physically transformed area is a small fraction of the project envelope and that terrain and road access, rather than turbine spacing, dominate variation in it (Denholm et al., 2009; Diffendorfer & Compton, 2014; Harrison-Atlas et al., 2022). For Greece specifically, Kati et al. (2023) quantify land take from wind

infrastructure and show that development concentrates on remote, higher-elevation natural terrain with access roads dominating the footprint, and Vlamakis et al. (2026) report a nationally representative infrastructure-based estimate of 0.33 ha per MW. This literature establishes the siting logic against which any claim of preference for burnt land must be assessed: turbines are placed where wind, slope and access permit, and that land is itself disproportionately dry upland.

2.1 Siting conflict, social acceptance and misinformation

Allegations of the kind tested here arise within a well-studied politics of renewable-energy siting. Social acceptance of renewable energy is conventionally analysed along socio-political, community and market dimensions (Wüstenhagen et al., 2007), and local opposition is now understood less as simple self-interest than as a response to disruptions of place attachment and perceived procedural unfairness (Devine-Wright, 2009; Rand & Hoen, 2017). Against that background, specific contrarian claims about wind energy circulate widely and cohere into a belief system rather than tracking the evidence for any individual claim. Winter et al. (2022) show that conspiracy beliefs predict opposition to wind farms and that this can be anticipated and defused, and Winter et al. (2024), surveying 6,008 respondents across three countries, find that agreement with diverse contrarian claims about wind farms is highly intercorrelated and best predicted by a conspiracist worldview rather than by education or science knowledge. The burn-to-build claim examined here has the structure such claims typically take: it attributes coordinated hidden intent to developers and authorities, it is empirically checkable in principle, and it has not previously been tested against a defensible base rate. Establishing what the spatial and temporal record does and does not show is therefore a contribution to the governance of siting conflict as well as to spatial analysis.

2.2 Mediterranean fire regimes and fuel classification

Separating a preference for burnt land from the background flammability of the terrain requires an explicit definition of fire-prone fuel. At the European scale, operational fuel mapping derives fuel types from land-cover classes combined with potential natural vegetation, an approach developed for pan-European fire-risk assessment (López et al., 2002) and used in the European Forest Fire Information System. More recently, the FirEUrisk hierarchical fuel classification provides a documented, multipurpose European fuel map built on the same principle of mapping land-cover classes to burnable fuel types (Aragoneses et al., 2023). Both schemes treat forest, sclerophyllous and transitional shrub, natural grassland and sparsely vegetated surfaces as burnable fuel classes, which is the basis for the fuel covariate specified in Section 4.5; the sensitivity of our results to that choice is reported in Section 5.2.

Across the Mediterranean most ignitions are of human origin, through negligence or deliberate acts, and their occurrence is driven by population density, distance to transport networks and settlements, the wildland-urban interface and agricultural activity rather than by any single land use (Ganteaume et al., 2013). In Greece, media, government and public opinion attributed the 2007 fires to arson serving real-estate and industrial interests, and fire has historically been used to encroach on public or disputed forest land (Palaiologou et al., 2021). Fire regimes have shifted from fuel-limited to drought-driven as rural abandonment increased fuel loads (Moreira et al., 2011; Pausas & Fernández-Muñoz, 2012); in Greece the long national record ties interannual burnt area mainly to summer weather (Koutsias et al., 2013), and large fires concentrate in a few extreme seasons (San-Miguel-Ayanz et al., 2013). Under Greek law burnt forest land must be declared reforestable and may not be put to another use (Hellenic Parliament, 2019, art. 117(3); Law 998/1979, art. 38), a protection whose interaction with renewable-energy siting is taken up in Section 6.3.

2.3 Use-availability designs and the modifiable areal unit problem

The question of whether a set of chosen locations is drawn preferentially from an available landscape is the use-availability problem of resource-selection analysis (Boyce et al., 2002; C. J. Johnson et al., 2006; D. H. Johnson, 1980; Manly et al., 2002). Inference in this framework depends critically on how availability is defined: Northrup et al. (2013) show that the extent and size of the availability sample materially change estimated coefficients, which is why the eligible universe used here is specified explicitly and probed across alternative thresholds. A second, equally established dependence concerns the unit of analysis. Results computed on areal units change when the zoning or scale of those units changes, a phenomenon known since Openshaw (1984) as the modifiable areal unit problem and demonstrated repeatedly in multivariate spatial analysis (Fotheringham & Wong, 1991) and landscape ecology (Jelinski & Wu, 1996).

https://doi.org/10.48088/ejg.s.str.17.1.399.424

The contrast reported in Section 5.2 between administrative licences and physical clusters of turbines is a concrete instance of this problem in infrastructure siting, and we treat it as such rather than as a novel observation.

3. Study area and data

The study covers the whole of Greece, a country with strong onshore wind resources on its mainland ridges and Aegean islands and with one of the highest wildfire burdens in the European Union (San-Miguel-Ayanz et al., 2024). Wind development and wildfire both concentrate in dry, elevated, sparsely built terrain, which is precisely why a naive spatial overlap is uninformative and a base-rate design is required. Greece records thousands of vegetation fires each year (Hellenic Fire Service, 2024), and its largest seasons burn well over one hundred thousand hectares (San-Miguel-Ayanz et al., 2024), concentrated in the dry summers and on the exposed upland terrain that also makes ridgelines attractive for wind development. Onshore wind capacity has grown rapidly over the study period as part of national decarbonisation targets, and independent quantification confirms that this growth concentrates on remote, higher-elevation natural terrain, with access roads dominating its land take (Kati et al., 2023). This shared geography is the confounding the present design is built to address, and the reason the question cannot be settled by inspecting a map of overlaps.

The unit of the wind fleet is the operational Greek Wind Power Station, equivalently a licensed wind farm, listed in the production-licence registry of the Regulatory Authority for Waste, Energy and Water (Regulatory Authority for Waste, Energy and Water [RAAEY], 2024), restricted to stations holding an operating licence (437 stations). Turbine geometry is taken from OpenStreetMap (2024), which for Greek wind turbines matches the industry count closely; of 2,995 mapped turbines, 2,958 are assigned to a station within 5 km and 37 are orphans. The 437 operational stations are the subset of a larger fleet of 508 licensed stations reported by industry that carry an operating rather than merely a production or installation licence; the remainder are excluded because they are not yet operational or lack the licence status from which a commissioning date can be derived. The 37 orphan turbines, more than 5 km from any station, are excluded from all farm-level analyses and never enter any of the three tests. Of the 437 operational stations, 398 have at least one turbine mapped in OpenStreetMap and 39 have none; since every spatial test locates a station through its turbines, those 39 cannot be placed and drop out. Those 398 stations, the “roughly 400” of Sections 5.2 and 6.1, are the pool for every spatial test; each test then uses the stations inside its own frame, which for the licence unit of Test B are those whose representative point lies in the eligible universe (292 for the hull centroid of Table 3, 315 for the mean-coordinate centroid of Table 6). Commissioning dates were resolved from public administrative acts to exact dates (from the Diavgeia transparency portal; 102 stations), to bounded intervals (113 stations), or to broader brackets from grid-operator records (117 stations); 105 stations remained unresolved, most of them either commissioned before 2008 or located on non-interconnected islands.

Fire perimeters come from the Copernicus European Forest Fire Information System (EFFIS) MODIS burnt-area product (European Forest Fire Information System, 2024), which maps fires above a nominal 30 ha threshold as dated polygons. The public layer covers approximately 2016 onward; perimeters for 2010 to 2015 were obtained through the EFFIS data-request service within the same product family. The merged 2010 to 2024 dataset comprises 1,644 perimeters whose areas sum to 607,005 ha, or 574,323 ha once overlapping perimeters are dissolved. The Hellenic Wind Energy Association (2025) reports 1,735 perimeters and 615,363 ha for 2008 to 2024 from the same EFFIS source. The two are of the same order, but that report does not state whether its total dissolves overlaps, so we do not treat the difference as a check on either.

Covariates are drawn from open products. Mean wind speed at 100 m is from the Global Wind Atlas (Global Wind Atlas, 2023); slope and aspect are derived from the Copernicus GLO-90 digital elevation model (European Space Agency & Airbus, 2022); land cover, including the fire-prone fuel classes used later, is from CORINE 2018 (European Environment Agency, 2019a); and protected status is from the Natura 2000 network (European Environment Agency, 2019b). All raster operations are performed on a common 100 m grid in the ETRS89 Lambert Azimuthal Equal-Area projection (EPSG:3035). Finally, to distinguish where fires ignited from the extent they eventually reached, we use NASA FIRMS satellite active-fire detections (NASA FIRMS, 2024), combining the MODIS and the VIIRS Suomi-NPP standard-processing archives (308,618 detections over Greece for 2010 to 2024); the earliest detection within 1 km of each burnt-area perimeter serves as an approximate ignition point and time (Section 4). Table 1 summarises the sources and their roles.

https://doi.org/10.48088/ejg.s.str.17.1.399.424

Table 1. Data sources and their roles in the analysis.

Layer	Product	Native resolution	Role
Turbines	RAAEY licences and OpenStreetMap	point	cases and events
Fire	EFFIS MODIS burnt areas, 2010 to 2024	~250 m	exposure
Wind	Global Wind Atlas, 100 m mean speed	~250 m	universe gate and covariate
Elevation	Copernicus GLO-90	~90 m	slope and aspect covariates
Land cover	CORINE 2018	100 m	exclusions and fuel covariate
Protected areas	Natura 2000	vector	covariate
Active fire	NASA FIRMS MODIS + VIIRS detections, 2010 to 2024	~375 m to 1 km	ignition points

Source: compiled by the author.

4. Methods

Our design combines three complementary tests, each addressing a different facet of the claim and each evaluated against the same eligible universe of wind-viable land (Figure 1). Test A asks, descriptively, whether fires tend to predate installation; it frames the ordering question but has no base rate. Test B asks whether wind farms are associated with burnt land more strongly than comparable wind-viable land would predict, using a use-availability case-control model; it is the core test of spatial preference. Test C asks whether a prior fire raises the subsequent probability of installation on eligible land, using a time-varying survival model in which fire enters as a time-dependent covariate; it is the core test of temporal direction. No single test is decisive alone: a spatial association without a time ordering points to shared static geography, whereas a genuine burn-to-build process should leave both a spatial signal and a positive, temporally ordered one. We therefore report all three across a common scale ladder and interrogate each for landscape confounding. The remainder of this section defines the eligible universe and then each test in turn.

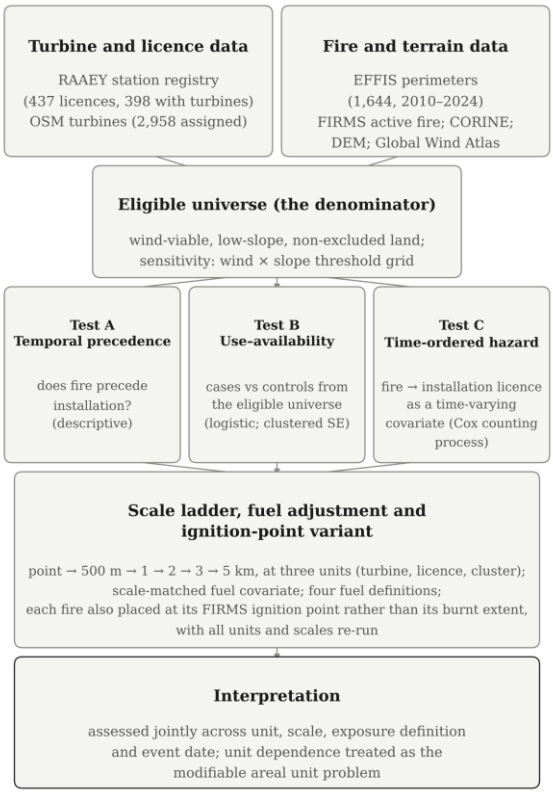


Figure 1. Research design. The eligible universe supplies the denominator for all tests; the three tests are run across the scale ladder and units with a scale-matched fuel covariate, then repeated with fire placed at its ignition point.

https://doi.org/10.48088/ejg.s.str.17.1.399.424

4.1 The eligible universe

The eligible universe is the set of wind-viable land cells that serves as the denominator for all base-rate comparisons; it is the "available" set against which used locations are contrasted. Both defining thresholds are calibrated to the existing fleet. The wind floor is set to the fifth percentile of Global Wind Atlas speed at existing turbines, 5.96 m/s, close to the conventional 6.0 m/s cut-off, and the slope ceiling is set to the ninety-fifth percentile of slope at existing turbines, 16.07 degrees. We further exclude open water, glaciers, and dense artificial surfaces (CORINE classes 511 to 523, 335, 111, 112, 123, 124, and 141), and we mask to Greek land defined as the intersection of Global Wind Atlas validity and CORINE data presence. The resulting primary universe covers 17,361 km², and 89.5% of mapped turbines fall inside it (2,680 of all 2,995 mapped turbines, the 37 orphans included; 2,644 of the 2,958 assigned turbines). Calibrating the universe to the fleet introduces a circularity, since cases help define the available set, which is why that share is high without being complete. We probe its consequences directly with a wind-by-slope threshold grid described below, and we list it explicitly among the limitations in Section 6.4, where we note that fleet calibration makes the available set resemble occupied land and can attenuate measured preference toward the null. Figure 2 shows the study area, the eligible universe, the burnt-area perimeters, and the turbine locations.

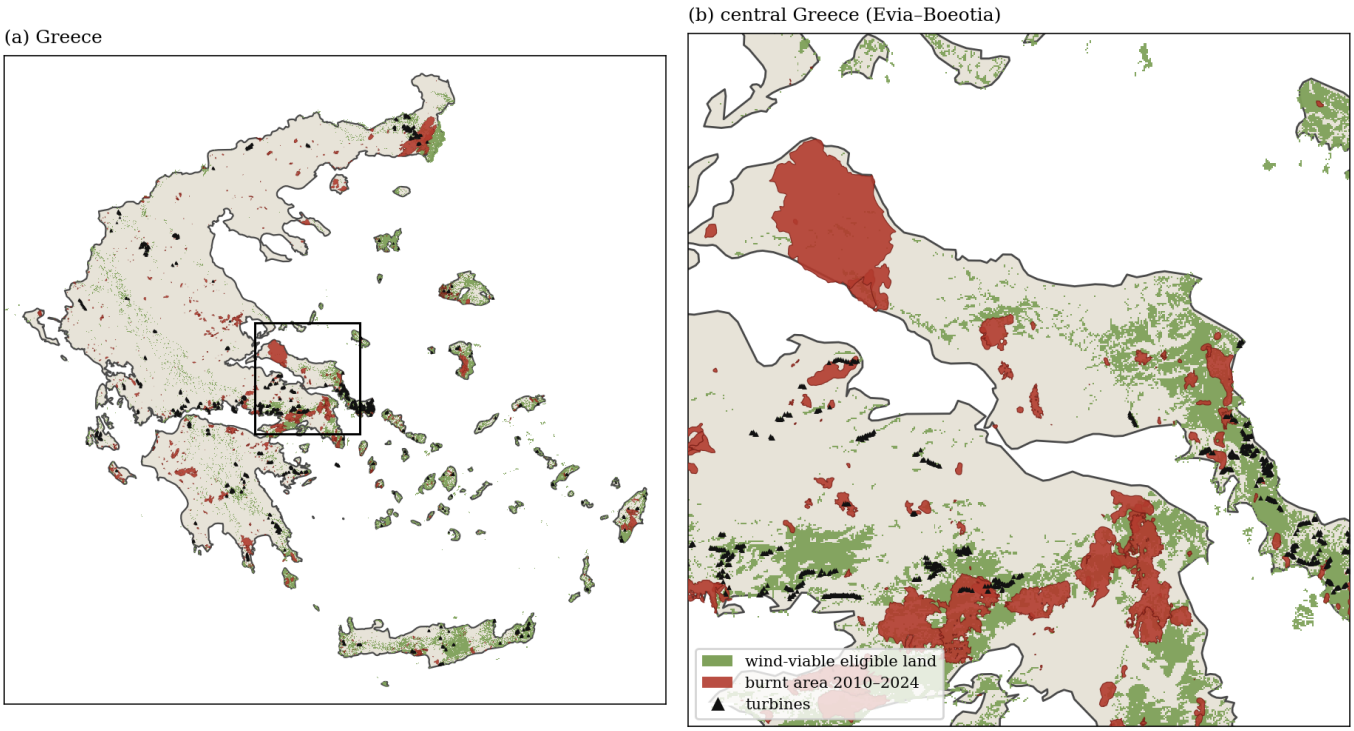


Figure 2. Study area. **(a)** Greece: national territory, wind-viable eligible land (green), burnt-area perimeters for 2010 to 2024 (red), and operational turbines (black triangles); the box marks the inset. **(b)** Central Greece (Evia and Boeotia), showing turbines, burns, and eligible land within fire-prone terrain. This area is shown because it has the densest co-occurrence of turbines, burnt area and eligible land in the country, and because the interleaved licence geometry discussed in Section 6.1 is legible there at readable scale.

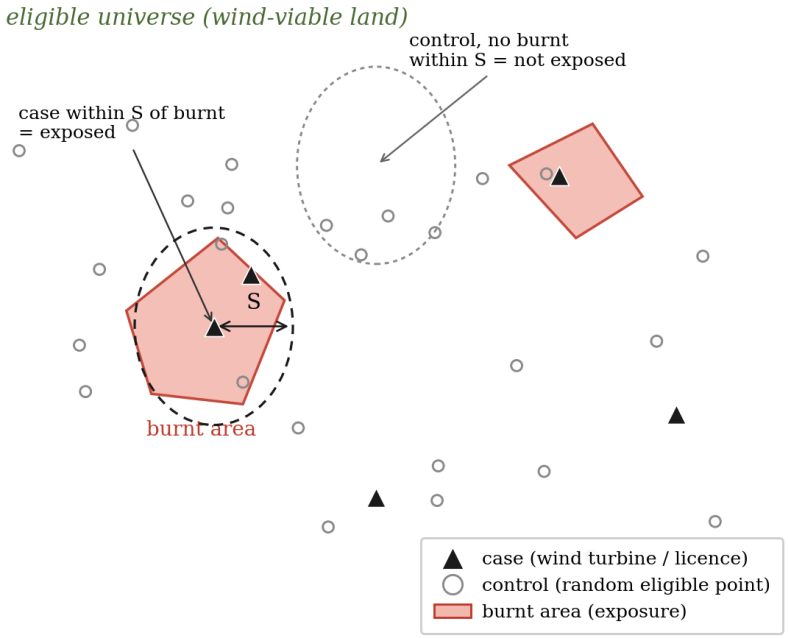
4.2 Test A: temporal precedence

For each station we form the convex hull of its turbines and buffer it at radii from 500 m to 5 km, then compare the dates of intersecting fires to the station's commissioning window, classifying each station as having a fire that predates installation, that is ambiguous because the fire date falls inside the commissioning window, that postdates installation, or as having none. Test A is purely descriptive and has no base rate; it is reported to show why raw counts, which grow with catchment size for every category simultaneously, cannot settle the question.

https://doi.org/10.48088/ejg.s.str.17.1.399.424

4.3 Test B: use-availability case-control

Test B asks whether wind sites fall near burnt land more often than comparable wind-viable land does. It contrasts cases, the wind sites, with controls, a random sample of the eligible universe, and asks whether being burnt-adjacent separates the two once landscape is accounted for (Figure 3). Controls are 30,000 cells drawn uniformly at random, without replacement, from the eligible universe, one point per cell; estimates are stable to this count.



Compare the burnt-exposure of cases vs controls by logistic regression, adjusting for wind, slope, elevation, aspect, protection, and fuel.

Figure 3. Test B as a use-availability case-control design. Cases (wind sites) are contrasted with controls drawn at random from the wind-viable eligible universe. A point is exposed if a burnt area lies within radius S of it. Logistic regression then asks whether burnt-adjacency distinguishes cases from controls once wind, slope, elevation, aspect, protection, and fuel are held constant.

The exposure is being burnt within the observation window: a case or control point lies within a radius S of any 2010 to 2024 perimeter. Each specification is a logistic regression, fitted with statsmodels (Seabold & Perktold, 2010), of case status on the burnt indicator plus wind speed, slope, elevation, aspect (as northness and eastness), and Natura status, with continuous covariates standardised.

We report two case definitions, because they answer different questions. In the turbine unit, cases are the 2,644 assigned turbines inside the universe (orphans excluded), with standard errors clustered by station; because it weights each project by its turbine count, this unit estimates the chance that an installed turbine lies near burnt land, and it is dominated by large developments. In the licence unit, cases are one representative point per RAAEY licence, the centroid of the convex hull of its turbines, restricted to the centroids inside the universe and weighting each project equally; this estimates the chance that a project is sited near burnt land.

Test B counts any overlap within the window, including fires that postdate installation, so the temporal direction is left to Test C. As an alternative exposure aimed at fire origin rather than extent, we replace the perimeter with an ignition point, the earliest FIRMS active-fire detection within 1 km of the perimeter, and repeat Test B at every unit.

4.4 Test C: time-varying survival

We follow eligible locations from 1 January 2010. The event is the issue of the installation licence, the last pre-construction permit, recovered from the Diavgeia transparency portal and matched to stations on company and site tokens. The location of a wind farm is largely fixed earlier, at the production licence and the environmental approval, so

the installation licence is not the siting decision itself but the latest milestone at which the location is still being confirmed, and the earliest milestone that could be recovered for most stations. For most farms the siting decision predates the fire record: 289 of the 412 stations with a dated production licence (70%) received it before 2010. The risk set is a random sample of the eligible universe, administratively censored at 31 December 2024. Commissioning is reported as a sensitivity analysis within the same framework. All units enter at the time origin; there is no delayed entry or left-truncation. Stations installed before 2010, and stations with unresolved dates, are prevalent rather than incident and are excluded from the event set. Events are stations whose matched licence date falls inside the window and whose turbines resolve to a footprint. The primary specification admits only stations whose earliest matching act is an original grant of an installation licence, giving 124 events, of which 87 fall inside the eligible universe. Admitting stations whose earliest matching act is an amendment or an extension, which dates the permit later than the original grant, gives 219 and 153. On the commissioning sensitivity the counts are 229 for all resolvable farms and 165 within the eligible universe. The risk set holds 30,000 control points drawn once at random from the eligible universe, the same draw that underlies the single-draw Test B tables, so each model follows the event stations together with 30,000 controls. Fire enters as a time-dependent covariate that switches from zero to one at the fire date, so that only fires preceding a given time contribute to the hazard and fires after the event never count. Events and controls are treated symmetrically as points sharing the same catchment. Models are fitted with lifelines (Davidson-Pilon, 2019) as a counting-process Cox model with a small ridge penalty (0.01) for numerical stability; standard errors are the model-based estimates and are not clustered, because each point enters the risk set once and control points share no station. Following standard practice for the Cox model (Cox, 1972), we test the proportional-hazards assumption for the burnt effect using an interaction between the burnt indicator and follow-up time. Test C is also re-estimated with fire entering at its ignition point and time rather than its perimeter, so that the temporal test concerns fire origins.

4.5 Scale ladder, fuel covariate, and robustness

Tests B and C are evaluated at radii from the point to 5 km, with the same radius applied to cases and controls so that the base rate moves with scale. To separate landscape fire-proneness from targeting, we add a scale-matched fuel covariate: the fraction of fire-prone natural fuel within the catchment, computed from eight CORINE 2018 classes: broad-leaved, coniferous and mixed forest (311, 312, 313), natural grassland (321), moors and heathland (322), sclerophyllous vegetation (323), transitional woodland-shrub (324), and sparsely vegetated areas (333). The moving window of the covariate is matched to the catchment radius, so that at each scale the contrast isolates the incremental contribution of fuel rather than the effect of adjustment against none; at the point scale a matched window would be a single 100 m cell, which measures the land-cover class of one cell rather than the composition around it, so that row uses a 500 m window. The covariate is computed independently of where fire actually occurred. For the licence-level association we replace comparisons across individual control draws with a permutation test using 1,000 label permutations implemented with scikit-learn (Pedregosa et al., 2011), and with a wind-by-slope threshold grid that rebuilds the eligible universe under nine combinations of wind floor and slope ceiling. In the gap analysis a short gap is defined as installation within three years of the fire.

Tables 3 and A1 (in the Appendix) report means over twenty independent control draws, with intervals combining within-draw and between-draw variance. The remaining tables are computed under a single fixed draw; at the primary cell the between-draw component is 2.2% of total variance, and the single-draw estimate for that cell is 1.40 against a twenty-draw mean of 1.34. The same offset applies to the licence row of Tables 6 and 7, which read 1.41 under the single draw against 1.35 over twenty draws for the same quantity, the licence represented by its mean-coordinate centroid. Single-draw and twenty-draw figures are therefore never compared with each other; each comparison in the paper is made within one convention, and Table A3 in the Appendix lists the convention behind every table.

One specification is primary and the remainder are sensitivity analyses of it. For Test B the primary specification is the licence unit at a 2 km catchment with the fuel covariate; for Test C it is the grant-basis installation-licence event restricted to the eligible universe. The scale ladder, the turbine and physical-cluster units, the alternative representative points, the wind-by-slope threshold grid, the alternative fuel definitions and the ignition-point exposure are sensitivity analyses: they re-estimate that same quantity under different assumptions rather than testing separate hypotheses, and no multiplicity correction is applied to them. Two further quantities reported in the Results are specified here. The size trend is a logistic regression, over the licences alone and with no control points, of an indicator for burnt land within 2 km on the base-ten logarithm of the licence's turbine count, together with the same standardised terrain, protection

and fuel covariates used in Test B; terciles of that logarithm give the accompanying descriptive rates. The expected count of post-licence fires is obtained, for each farm with a production-licence date and a three-year post-licence window falling inside the fire record, as the probability of at least one fire in its own catchment during that window under the catchment's empirical annual fire rate. Summing those probabilities over farms gives the expectation against which the observed count is compared; the reported tail probability is one-sided under the corresponding Poisson model.

5. Results

5.1 Temporal precedence

Burnt-before farm counts grow with catchment size, from 17 at 500 m to 95 at 5 km, but so do fires of every other category (Table 2); by 5 km 211 of the 302 farms (70%) have a fire within range. A raw count therefore cannot distinguish preference from the background fire rate, which is exactly the base-rate problem the remaining tests are designed to overcome.

Table 2. Test A, farm-level temporal precedence for the 302 stations with mapped turbines and a resolved commissioning date; the 96 unresolved stations with mapped turbines are reported separately.

Catchment	Predates	Ambiguous	Postdates	No fire
hull + 500 m	17	9	41	235
hull + 1 km	31	12	47	212
hull + 2 km	55	19	67	161
hull + 3 km	71	21	78	132
hull + 5 km	95	28	88	91

Source: author's analysis of EFFIS and RAAEY data.

5.2 Spatial association

The spatial result depends on the unit of analysis (Table 3, Figure 4). Under the turbine unit, which weights each project by its number of turbines, no significant burnt association appears at any scale, and the small excess that remains disappears once the fuel covariate is added. Under the licence unit, weighting each licensed project equally, a significant landscape-scale association emerges: the burnt odds ratio is 1.60 at 2 km, peaking at 1.66 at 3 km and easing to 1.62 at 5 km. Adding the fuel covariate explains roughly two-fifths of this but leaves a residual odds ratio of 1.34 at 2 km and 1.37 at 3 km, both statistically significant, and 1.28 at 5 km, which is not; at 1 km the fuel covariate removes it entirely. This residual does not depend on how fire-prone fuel is defined. Re-estimating the 2 km licence-level model under three alternative definitions gives odds ratios of 1.54 for a narrow woody definition that drops grassland and sparsely vegetated land, 1.50 when agricultural classes are added, and 1.34 for a definition aligned with the EFFIS and FirEUrisk European fuel maps, against 1.40 for the definition used here (Table A2 in the Appendix). All four are significant, and all four are computed under the single control draw so that the comparison between definitions is like for like. The definition used here, at 1.40, lies between the EFFIS and FirEUrisk-aligned definition (1.34) and the other two (1.50 and 1.54), so it is neither the lowest nor the highest of the four, and the residual remains significant under all four (1.34 to 1.54). The point scale is null in both units. As shown below, this licence-level association does not survive a physical definition of the unit; Section 6.1 examines what that dependence does and does not imply, since the licences concerned are, in many clusters, held by different developers.

https://doi.org/10.48088/ejg.s.str.17.1.399.424

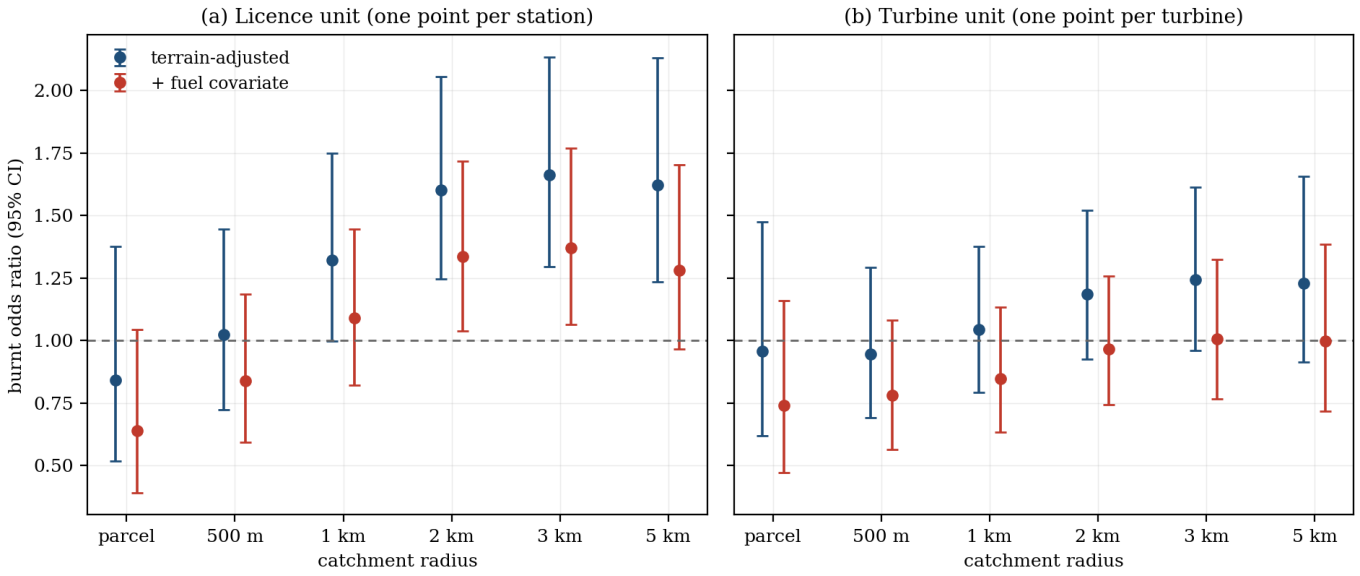


Figure 4. Test B burnt odds ratio with 95% confidence intervals, terrain-adjusted and with the fuel covariate added, across catchment radius. (a) Licence unit: a significant 2 to 3 km association with a residual near 1.35 after fuel, which depends on the choice of spatial unit (see Section 5.2). (b) Turbine unit: null and fully absorbed by fuel. The dashed line marks no effect.

Table 3. Test B burnt odds ratio with 95% confidence intervals, by unit and scale. Both columns for each unit adjust for wind speed, slope, elevation, aspect and protected status; the second adds the scale-matched fire-prone fuel covariate (Section 4.5). Cases are the 2,644 turbines and 292 licences within the eligible universe, against 30,000 controls per draw; estimates are means over 20 independent control draws (seeds 1 to 20), with intervals combining within-draw and between-draw variance.

Scale	Turbine, terrain-adjusted	Turbine, + fuel	Licence, terrain-adjusted	Licence, + fuel
point	0.96 (0.62–1.48)	0.74 (0.47–1.16)	0.84 (0.52–1.38)	0.64 (0.39–1.05)
500 m	0.95 (0.69–1.29)	0.78 (0.56–1.08)	1.02 (0.72–1.45)	0.84 (0.59–1.18)
1 km	1.04 (0.79–1.38)	0.85 (0.63–1.13)	1.32 (1.00–1.75)	1.09 (0.82–1.45)
2 km	1.19 (0.93–1.52)	0.97 (0.74–1.26)	1.60 (1.25–2.06)	1.34 (1.04–1.72)
3 km	1.24 (0.96–1.61)	1.01 (0.77–1.32)	1.66 (1.30–2.14)	1.37 (1.06–1.77)
5 km	1.23 (0.91–1.66)	1.00 (0.72–1.38)	1.62 (1.23–2.13)	1.28 (0.97–1.70)

Source: author's analysis.

Within the licence unit the association is small and its strength depends on how the licence is reduced to a point. A permutation test on the 2 km fuel-adjusted estimate, using 1,000 label permutations under each of six independent control draws, gives p between 0.037 and 0.095 with a median of 0.074, so permutation inference places the observed effect at the edge of the null rather than clearly outside it. Its magnitude is similar across the wind-by-slope threshold grid (Table 4), where the fuel-adjusted odds ratio ranges from 1.25 to 1.39 and is significant in eight of the nine universe definitions, the exception being wind ≥ 5.5 m/s with slope ≤ 18° at p = 0.067 (areas and case counts in Table 5). It is not stable across the choice of representative point for each licence. Over the same twenty control draws the fuel-adjusted 2 km odds ratio is 1.34 for the primary hull-centroid point and 1.35 for the mean-coordinate centroid, both significant, but 1.22 for the turbine nearest the centroid and 1.22 for a randomly chosen turbine per licence, neither of which is significant (p = 0.105 and p = 0.112). The association is therefore strongest for a synthetic point that no turbine occupies

and weakest when a licence is represented by one of its actual machines, which is consistent with the licence-level residual reflecting the geometry of the unit rather than a property of the sites; Section 6.1 tests that reading directly, against the ownership of the licences themselves.

Table 4. Licence-level Test B at 2 km, fuel-adjusted burnt odds ratio with 95% confidence intervals, across eligible-universe thresholds. All estimates in this table use the single fixed control draw; see Section 4.5.

	slope ≤ 15°	**slope ≤ 18°**	**slope ≤ 20°**
wind ≥ 5.5	1.38 (1.07–1.77)	1.25 (0.98–1.59)	1.27 (1.01–1.60)
wind ≥ 6.0	1.35 (1.04–1.73)	1.35 (1.06–1.72)	1.30 (1.03–1.65)
wind ≥ 6.5	1.39 (1.07–1.80)	1.32 (1.03–1.69)	1.28 (1.01–1.63)

Source: author's analysis.

Table 5. Eligible-universe area (km²) and number of licence cases for each threshold in Table 4.

	slope ≤ 15°	**slope ≤ 18°**	**slope ≤ 20°**
wind ≥ 5.5	21,524 (n = 295)	25,199 (n = 326)	27,291 (n = 345)
wind ≥ 6.0	15,885 (n = 281)	18,726 (n = 311)	20,344 (n = 329)
wind ≥ 6.5	11,608 (n = 265)	13,782 (n = 291)	15,023 (n = 307)

Source: author's analysis.

The association is, however, specific to the administrative licence as the unit. When the same turbines are grouped into physical clusters by spatial proximity, independently of licence boundaries, the fuel-adjusted 2 km association disappears at every clustering distance (Table 6): the odds ratio lies between 0.91 and 0.99 and is never significant, from 300 m clustering (1,040 clusters) to 3 km clustering (163 clusters). It is also null at the turbine unit. The signal thus appears only when the roughly 400 administrative licences are treated as independent units, and vanishes under both finer (turbine) and coarser (physical-cluster) groupings. Development size may be part of why the turbine unit is null. Larger developments are somewhat less fire-adjacent: the share of licences with a fire within 2 km falls from 0.50 in the smallest size tercile to 0.45 in the middle and 0.34 in the largest, and burnt-adjacency declines at an odds ratio of 0.64 per tenfold increase in turbine count (95% confidence interval 0.35 to 1.19, p = 0.158). The trend runs in the direction opposite to the burn-to-build claim, but it is not statistically significant, so we report it without relying on it.

One candidate explanation, suggested by the interleaved and subdivided licence geometry seen on the licence maps (Section 6.1), is that developments in fire-prone terrain are divided into more, spatially overlapping licences, so that weighting each licence equally would over-count the shared fire-prone ground, with physical grouping removing both the over-counting and the association. This is a hypothesis about who holds the licences, and Section 6.1 tests it against the licence register rather than assuming it.

5.3 Proximity to fire ignitions

The exposure used so far is the extent of each burnt area, so a location counts as near a fire even when the fire spread to it from a distant origin. Using instead the ignition point, the earliest satellite active-fire detection within 1 km of each perimeter, moves the test toward where fires start, within the positional accuracy of the detections (Section 6.4). Ignition points were recovered for 1,590 of the 1,644 perimeters (97%). Against them the fuel-adjusted 2 km association is null at every unit (Table 7): the odds ratio is 0.91 for turbines, 1.17 for the administrative licence, and 0.94 for physical clusters, none significant. At the licence unit, on the same single control draw, the 1.41 (1.11 to 1.80) seen against fire extent becomes a weaker and no longer significant 1.17 (0.87 to 1.57) once the fire is placed at its origin rather than its edge; the two intervals overlap substantially, so this is a weakening of the administrative-unit signal rather than evidence of a difference between the two exposures.

Table 6. Fuel-adjusted burnt odds ratio at 2 km when turbines are grouped into physical clusters by proximity (one point per cluster), compared with the administrative licence unit (represented by its mean-coordinate centroid). The 398 licences are the operational stations with at least one mapped turbine, of the 437 in the registry; in every row the cases are the groups whose representative point lies inside the eligible universe, given in parentheses. All estimates in this table use the single fixed control draw; see Section 4.5.

Grouping	Distance	Groups (in universe)	Odds ratio (95% CI)	p
Administrative licence	—	398 (315)	1.41 (1.11–1.80)	0.005
Physical cluster	300 m	1,040 (884)	0.97 (0.82–1.13)	0.68
Physical cluster	500 m	561 (484)	0.95 (0.77–1.17)	0.64
Physical cluster	1,000 m	306 (248)	0.95 (0.71–1.26)	0.70
Physical cluster	1,500 m	233 (183)	0.99 (0.71–1.37)	0.93
Physical cluster	2,000 m	199 (149)	0.95 (0.67–1.36)	0.80
Physical cluster	3,000 m	163 (118)	0.91 (0.60–1.36)	0.64

Source: author's analysis.

Table 7. Test B at 2 km, fuel-adjusted, against fire ignition points (earliest FIRMS detection within 1 km of each perimeter) versus burnt-area extent; the physical-cluster row uses the 1 km clustering of Table 6. All estimates in this table use the single fixed control draw; see Section 4.5.

Unit	Near ignition point: OR (95% CI), p	Near burnt extent: OR (95% CI), p
Turbine	0.91 (0.80–1.04), 0.16	1.01 (0.78–1.30), 0.95
Administrative licence	1.17 (0.87–1.57), 0.29	1.41 (1.11–1.80), 0.005
Physical cluster	0.94 (0.65–1.35), 0.73	0.95 (0.71–1.26), 0.70

Source: author's analysis of FIRMS and EFFIS data.

5.4 The time-ordered test

The choice of event date matters, because commissioning postdates the siting decision by several years. We therefore take the installation licence, the latest pre-construction milestone (Section 4.4), as the event, and report commissioning as a sensitivity. Installation-licence issue dates were recovered from the Diavgeia transparency portal and matched to stations on company and site (245 matched stations, 142 of them based on an original grant act); the reliability of that linkage is examined below. Table 8 collects the hazard ratios under every event definition.

On the installation-licence event the association is null in every specification: 1.06 (95% confidence interval 0.86 to 1.29, p = 0.60) on 124 grant-basis events and 1.05 (0.85 to 1.29, p = 0.65) on the 87 of those within the eligible universe, and 1.10 (p = 0.34) on 219 events and 1.13 (p = 0.25) on 153 when amendment-dated matches are included. Proportional hazards holds on this event: the interaction between the burnt indicator and follow-up time is −0.0028 per year of follow-up (p = 0.75) for grant-basis events and −0.0006 per year (p = 0.95) within the eligible universe, so there is no front-loaded post-fire effect.

The commissioning sensitivity, run on the same design with commissioning as the event, behaves differently and is reported so the comparison is checkable. At 2 km it gives 1.12 (p = 0.22) on 229 resolvable farms and 1.15 (p = 0.16) on the 165 within the eligible universe, both null; adding an interaction between the burnt indicator and follow-up time raises both to 1.37 (p = 0.001) and 1.32 (p = 0.007), and proportional hazards fails in each (p < 0.001). Run symmetrically on both event sets, the two sets agree; what changes the estimate is the interaction term, not the event set. Commissioning is therefore less suitable as a temporal basis: the proportional-hazards assumption fails on that event in every

specification in which it was tested, and the front-loading it implies is probably an artefact of dating the event years after the siting decision, although the significant hazard ratios of the interaction models remain a result we cannot explain. Re-dating to the installation licence removes the problem: on that event the estimate is null and proportional hazards holds.

Re-estimated against ignition timing rather than perimeter timing, with the exposure defined as an ignition point within 2 km before the event, the hazard ratio on the installation-licence event is null in every specification, between 1.02 and 1.05 with $p \geq 0.73$ and proportional hazards holding, and it is likewise null on the commissioning event (Table 8), so no time-ordered association with fire origins is present under either event.

Table 8. Test C hazard ratio for a prior fire within 2 km, by event definition and specification. All models follow the event stations together with 30,000 control points drawn once from the eligible universe (Section 4.4). Rows labelled fire at ignition time replace the burnt-area perimeter with the earliest FIRMS detection within 1 km of it (Section 4.3). The proportional-hazards column gives the burnt × follow-up-time interaction, per year of follow-up, where it was tested. The grant-basis installation-licence event restricted to the eligible universe is the primary specification.

Event definition	Specification	Events	Hazard ratio (95% CI)	p	Proportional hazards
Installation licence, grant basis	all resolvable farms	124	1.06 (0.86–1.29)	0.603	holds; burnt × time −0.0028 (p = 0.753)
Installation licence, grant basis	within eligible universe	87	1.05 (0.85–1.29)	0.652	holds; burnt × time −0.0006 (p = 0.947)
Installation licence, amendment-dated included	all resolvable farms	219	1.10 (0.91–1.33)	0.338	not tested
Installation licence, amendment-dated included	within eligible universe	153	1.13 (0.92–1.38)	0.246	not tested
Commissioning (sensitivity)	all resolvable farms, no interaction	229	1.12 (0.93–1.35)	0.221	fails (p < 0.001)
Commissioning (sensitivity)	within eligible universe, no interaction	165	1.15 (0.95–1.39)	0.165	fails (p < 0.001)
Commissioning (sensitivity)	all resolvable farms, with burnt × time	229	1.37 (1.13–1.67)	0.001	fails (p < 0.001)
Commissioning (sensitivity)	within eligible universe, with burnt × time	165	1.32 (1.08–1.62)	0.007	fails (p < 0.001)

https://doi.org/10.48088/ejg.s.str.17.1.399.424

Event definition	Specification	Events	Hazard ratio (95% CI)	p	Proportional hazards
Installation licence, grant basis, fire at ignition time	all resolvable farms	124	1.03 (0.79–1.34)	0.830	holds; burnt × time −0.0087 (p = 0.530)
Installation licence, grant basis, fire at ignition time	within eligible universe	87	1.04 (0.79–1.36)	0.784	holds; burnt × time −0.0034 (p = 0.808)
Installation licence, amendment-dated included, fire at ignition time	all resolvable farms	219	1.02 (0.80–1.30)	0.887	not tested
Installation licence, amendment-dated included, fire at ignition time	within eligible universe	153	1.05 (0.81–1.36)	0.731	not tested
Commissioning, fire at ignition time	all resolvable farms	229	1.04 (0.82–1.32)	0.728	not tested
Commissioning, fire at ignition time	within eligible universe	165	1.10 (0.86–1.41)	0.461	not tested

Source: author's analysis.

The reliability of that linkage bears on how much weight the result can carry. Acts name the licence holder and the site in free text rather than by registry identifier, so stations were matched on agreement of both company and site tokens. Of the 245 matched stations, 163 rest on more than one matching token in at least one field and 82 on the minimal criterion of one company and one site token. Two checks support the linkage. Dates behave as the milestone should: for the 82 stations with a bounded commissioning window, 96% of installation dates precede the midpoint of that window, the median lead is 2.0 years, and three cases run the other way. All three carry bounded rather than exact commissioning dates, so the ordering there is uncertain in both directions. And the matched set spans the study period evenly rather than clustering in years where the portal is best populated. The 192 unmatched stations are not missing at random, since acts that omit either the company name or the site cannot be linked, so the temporal test speaks to the matched subset rather than to the whole fleet; we report this as a limitation in Section 6.4 and give the matching code and the harvested acts in the data archive.

5.5 Fire-to-installation gap and post-licence fire counts

For farms that burnt before installation, the interval between fire and installation is long, with a median of 6 to 7 years, dominated by the five-to-ten-year bin and extending to 12 years (Table 9, Figure 5). Short gaps are rare partly by construction: most siting predates the 2010 start of the record, so a fire that cleared a site before it was chosen would usually fall outside the record; the gaps are measured to commissioning, which follows siting by years; and fires below about 30 ha are not mapped. The length of the observed gaps is therefore weak evidence on its own.

The raw ordering of licence and fire dates is largely a timeline artefact: most fires fall after the production licence for reasons that have nothing to do with siting. Greek production licences were mostly issued before the fire record begins in 2010 (289 of the 412 dated licences, Section 6.4), and the installation licence follows the production licence by a median of 9.5 years among the 140 grant-basis installation licences with a dated production licence, with 47% of gaps exceeding ten years. The EFFIS perimeters used here map only fires above about 30 ha and number roughly 110

per year, a small fraction of the roughly 9,600 forest-fire incidents reported in Greece each year, an average over the 162,961 incidents recorded between 2008 and 2024 (Hellenic Fire Service, 2024, as cited in Hellenic Wind Energy Association, 2025). Over a post-licence period of that length, an incidental perimeter within a few kilometres of a site is common enough that the raw ordering of licence and fire dates carries little information.

We therefore tested the temporal profile most directly implied by the claim, comparing the number of farms with a fire in the three-year window after the production licence against the number expected from the empirical fire rate in the same catchment (Table 10). At a 1 km catchment 14 farms are observed against 8.7 expected (Poisson $P(X \geq 14) = 0.058$; binomial $p = 0.075$), and at 2 km 21 against 14.6 ($P = 0.069$; binomial $p = 0.094$). The observed count exceeds expectation at every catchment, by 44% at 2 km rising to 73% at 500 m. The excess is not significant at conventional thresholds at any catchment, and the smallest one-sided tail probability is 0.058 at 1 km, but neither is it negligible; we report it as a weak and unresolved signal rather than as evidence either way. Tables 9 and 10 are different calculations on different sets: Table 9 counts, among the stations installed inside the fire record that had an earlier catchment fire, how long before installation the fire fell, whereas Table 10 runs over the 129 farms with a production-licence date and a post-licence window inside the record and asks how many saw a fire in the three years after the licence. Table 2 differs from both: it classifies all 302 resolved stations, including those installed before 2010, and counts a fire as predating installation when it precedes the lower bound of the commissioning window rather than its midpoint, so its predates column is not comparable with the n of Table 9.

Table 9. Fire-to-installation gap and licence ordering for burnt-before farms; a short gap is installation within three years of the fire. Rows count stations whose installation date, taken as the midpoint of the commissioning window, falls inside the 2010 to 2024 fire record (229 stations) and that have at least one earlier fire in the catchment, so n varies with the catchment. The fire after/before licence column counts only those with a production-licence date (11 of 12, 19 of 20 and 32 of 35), which is why its entries sum to less than n; the last column counts the stations with a short gap whose fire also fell after the production licence. Section 5.5 explains how these counts relate to Tables 2 and 10.

Catchment	n	Median gap (yr)	Fire after / before licence	Short gap, fire after licence
hull	12	6.8	11 / 0	3
500 m	20	6.8	19 / 0	4
1 km	35	6.1	30 / 2	11

Source: author's analysis.

Table 10. Farms with a fire in the three-year window after the production licence, observed against the number expected from the empirical fire rate in the same catchment. The 129 farms are those with a mapped turbine hull, a production-licence date, and a post-licence window falling inside the 2010 to 2024 fire record, out of 398 with a hull and 373 of those with a licence date. Expected counts are the sum over farms of the probability of at least one catchment fire in the window, given each farm's own fire rate. The Poisson tail probability is one-sided and is computed from the unrounded expected count, which the table shows rounded to one decimal; the binomial p-value is the two-sided exact test of the observed count against the 129 farms with success probability equal to the expected count divided by 129. Catchments are the turbine convex hull buffered by the stated distance, as in Table 9.

Catchment	Farms in test set	Observed	Expected	Poisson $P(X \geq$ observed); binomial p
hull	129	5	3.3	0.244; 0.393
500 m	129	9	5.2	0.082; 0.109
1 km	129	14	8.7	0.058; 0.075
2 km	129	21	14.6	0.069; 0.094

Source: author's analysis.

https://doi.org/10.48088/ejg.s.str.17.1.399.424

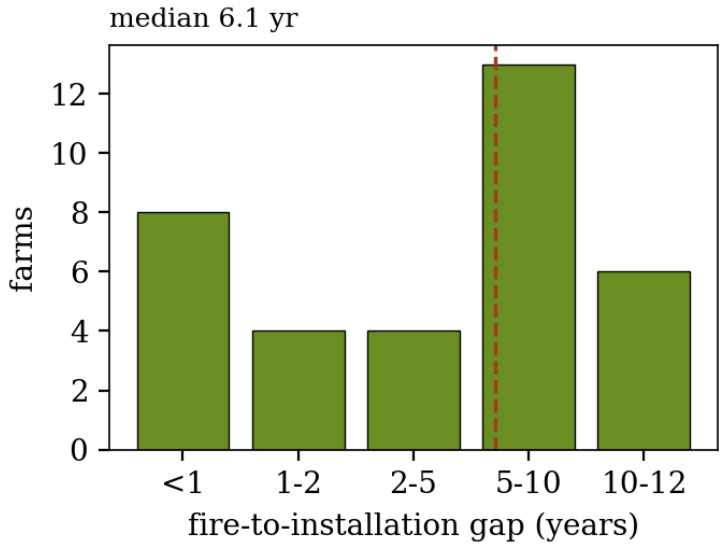


Figure 5. Fire-to-installation gap for burnt-before farms (1 km catchment, n = 35); the dashed line marks the median of 6.1 years.

6. Discussion

The point scale is null in every test, so there is no evidence that specific burnt plots were selected for specific turbines. What survives is a landscape-scale spatial association, and its character can now be described precisely.

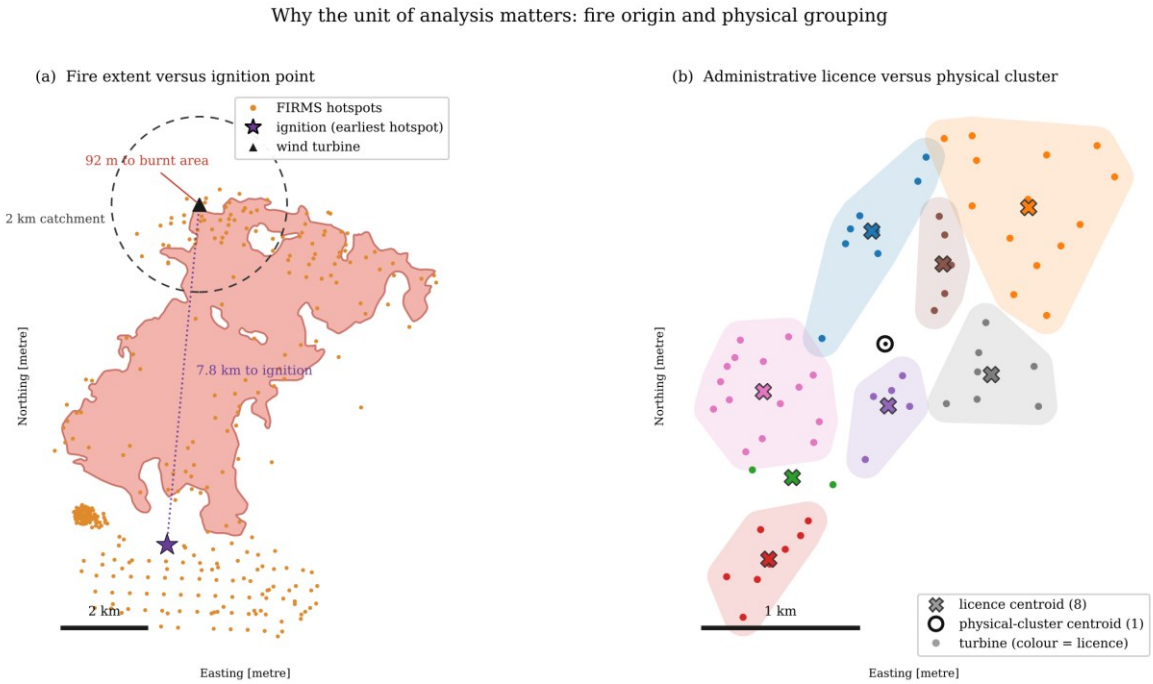


Figure 6. Unit of analysis and exposure definition, on real data. **(a)** Fire extent versus ignition point: a burnt-area perimeter with its FIRMS hotspots, the earliest marked as the ignition; the nearest turbine lies 92 m from the burnt extent but 7.8 km from the ignition. **(b)** Administrative licence versus physical cluster: eight interleaved RAAEY licences, turbines coloured by licence and licence centroids marked X, occupy one physical development whose single centroid is ringed.

https://doi.org/10.48088/ejg.s.str.17.1.399.424

6.1 The unit of analysis

The landscape-scale association depends on how the unit of analysis is defined, and that dependence is itself the finding. Two observations frame it. First, weighting by turbine count removes it: the turbine unit weights each project by the number of turbines it contains, is dominated by large developments, and is null at every scale (Table 3). Second, grouping turbines physically rather than administratively also removes it: at every clustering distance from 300 m to 3 km the fuel-adjusted odds ratio is close to one and non-significant.

The association survives only at the level of the roughly 400 RAAEY licences, where it persists under several universe and fuel definitions, though permutation inference places it near the edge of the null and it weakens when a licence is represented by an actual turbine rather than a centroid; it is bracketed on both sides by null results at finer and coarser physical groupings. One reading of that pattern would be administrative: if developments in fire-prone terrain were subdivided into more interleaved licences than developments elsewhere, counting each licence equally would over-represent the shared fire-prone ground, an over-representation that physical grouping dissolves (Figure 6b). We therefore checked who holds these licences, using the holder recorded in the licence register. Holders are grouped into corporate groups by ownership as it stood when each licence was issued, not as it stands now, since grouping by present ownership would impose a later corporate structure on an earlier process.

Two 2024 acquisitions are affected by that choice, and it turns out to be immaterial: under either convention 52 of the 77 multi-licence clusters (clusters formed by DBSCAN at 1 km, the 1,000 m row of Table 6), 68%, contain two or more distinct groups, because the acquired and acquiring groups hold licences in the same cluster in only two cases, both of which already contain a third, unrelated holder. In many clusters, therefore, adjacent licences are held by different developers rather than being one developer's subdivision of a project; Figure 7 shows a representative case, in which fourteen licences on a single ridge system are held by eleven distinct groups.

Special-purpose vehicles (SPVs) are merged into their parent group wherever that parent could be established, which is the conservative direction, since merging can only lower the multi-developer share. Attribution was verified for the largest such series, the seventeen vehicles of one developer's complex in southern Evia, which a single administrative act names as one project sharing one interconnection; treating them as separate holders would have overstated the share by three percentage points. Because the licence register records the holder rather than the ultimate owner, and because comparable series may exist for other groups, 68% should be read as an upper bound. The licence therefore represents a distinct administrative and, in many clusters, developer-level decision unit, and the licence-level association cannot be dismissed as bookkeeping. Both units are meaningful: the licence captures the decision of an individual developer, whereas the physical cluster captures the terrain a development occupies, and the association is present at one and absent at the other. This is the modifiable areal unit problem in its classic form (Fotheringham & Wong, 1991; Openshaw, 1984), and we report both units rather than privileging either. What it does not settle is whether burnt ground is preferred, which the ignition-point analysis addresses more directly, within the positional limits noted in Section 5.3.

6.2 Interpretation

The licence-level residual is small; it persists across the fuel and universe definitions we tested, but it sits at the edge of the null under permutation inference and it weakens and loses significance when a licence is represented by one of its own turbines rather than by a centroid. It does not survive a change in the unit of analysis, and it does not survive a change of exposure: placing each fire at its ignition point rather than at its extent leaves no significant association at any unit, the licence included (Table 7). Proximity to where a fire began, rather than to the extent it eventually reached, is the exposure the alleged mechanism implies, so this is in principle the more direct test of the two. A satellite detection, however, locates an ignition only to within a few hundred metres to about a kilometre, a sizeable fraction of the 2 km catchment, so its null is less precise than the perimeter result it accompanies. What is left is that wind farms sit on fire-prone terrain. We read this as shared occupancy of dry, exposed, sparsely built uplands by wind resource and fire rather than as burnt ground being sought out; this is an interpretation consistent with the covariate structure below, not a directly tested result. Our measured covariates behave as expected, and Table A1 in the Appendix reports them in full. At the licence unit and 2 km, wind speed (odds ratio 1.92, 95% confidence interval 1.78 to 2.08) and fuel (2.61, 2.12 to 3.22) are strong positive predictors, while slope (0.65, 0.56 to 0.74) and protected status (0.39, 0.30 to 0.53) are strong negative ones. Elevation and the two aspect terms are not significant. These covariates capture much of the

shared geography. The residual that remains is present at the licence unit and absent at the turbine and physical-cluster units, and the present data cannot separate residual geographic confounding, siting variables we do not observe such as grid connection, road access and land ownership, and developer-level selection of landscapes that also burn. We decline to choose between them. For the specific claim, that fires are set in order to build, the evidence is unsupportive on most tests: the point scale is null, the turbine and physical-cluster scales are null, the time-ordered hazard is null once the event is dated at the installation licence, with no front-loaded structure, and the fire-to-installation gaps are long; the exceptions, which we do not set aside, are the weak post-licence excess of Section 5.5 and the commissioning interaction models of Section 5.4. A mechanism in which fires were intentionally set to facilitate construction would produce short, consistent fire-to-installation intervals and a stable positive temporal association; we observe neither, with the caveat that short gaps are under-observed by construction, since most siting predates the 2010 start of the record, the gaps run to commissioning rather than to siting, and fires below about 30 ha are omitted, so the time-ordered test rather than the gap lengths carries the weight of this conclusion. Placing each fire at its ignition point rather than its extent weakens the licence-unit signal to non-significance (Section 5.3) and leaves the time-ordered test null, so we find no evidence that turbines are nearer to where fires start than random wind-viable land (Figure 6a).

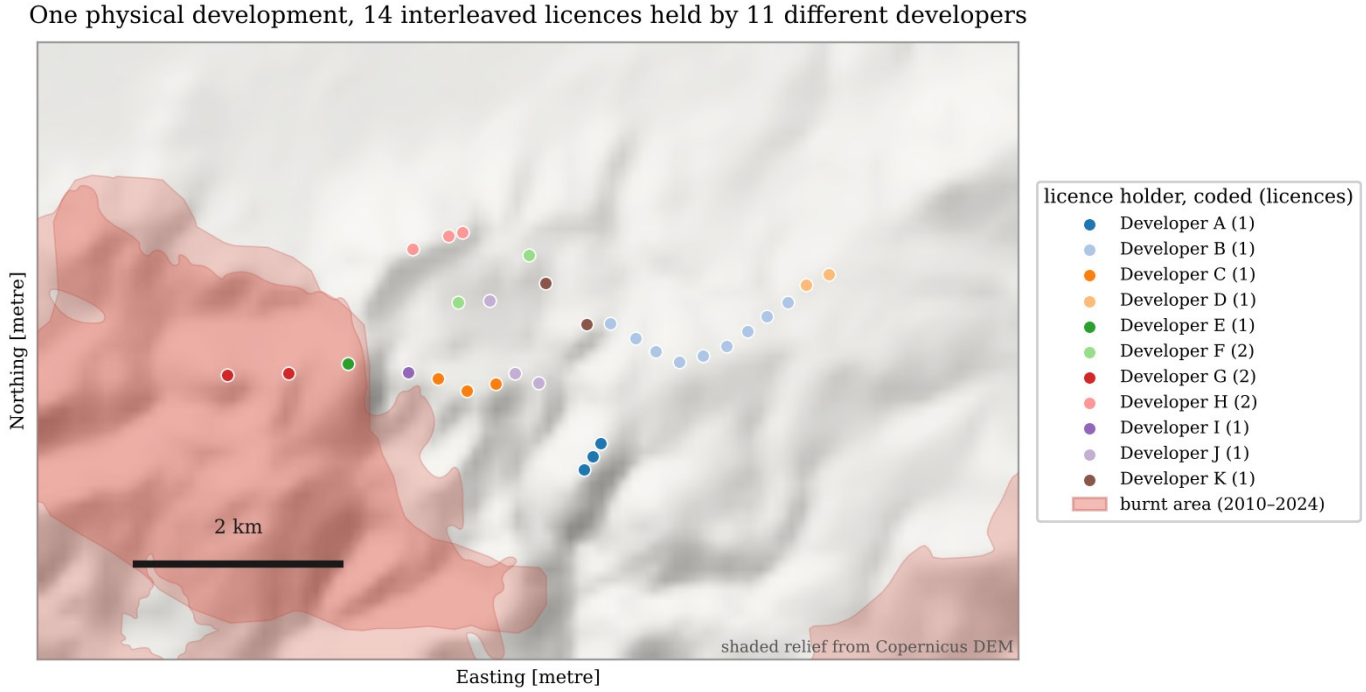


Figure 7. Interleaved licences of different developers within one physical development. Fourteen RAAEY licences held by eleven distinct corporate groups, shown as coded holders (Developer A to K), occupy a single contiguous ridge system; turbines are coloured by licence holder, and licence counts per holder are given in the legend.

6.3 Relation to prior work

The peer-reviewed characterisation of Greek wind siting (Vlamakis et al., 2026) reports a nationally representative land-use intensity of 0.33 ha per MW and finds development concentrated on low-vegetation upland terrain, which is consistent with the terrain preferences our covariates recover. On the fire claim itself, our conclusion converges with, and strengthens the basis for, earlier analyses that found no correlation between wind farms and burnt land (Hellenic Wind Energy Association, 2025; Vlamakis et al., 2025). All three are authored from within the national wind-industry association, a provenance we state plainly, and only the first is peer reviewed. We therefore benchmark additionally against independent peer-reviewed estimates of wind land take and siting (Denholm et al., 2009; Diffendorfer & Compton, 2014; Kati et al., 2023), while grounding our conclusion in a comparison against the land where turbines could actually be placed, which the earlier footprint percentages did not provide. A recent quantitative analysis of the same question also reports, from fire-service ignition records for 2020 to 2024, no case of a wind turbine installed inside a burnt area after the fire started (Hellenic Wind Energy Association, 2025); our independent satellite ignition analysis,

which asks the different question of proximity to where fires started and locates each ignition only to within about a kilometre, reaches the same null across the full 2010 to 2024 period.

The legal regime bears on how the claim should be read. Burnt forest land must be declared reforestable and may not be put to another use (Hellenic Parliament, 2019, art. 117(3); Law 998/1979, art. 38), yet the forest law also exempts renewable-energy generation works from the general ban on interventions in forest land (Law 998/1979, art. 45(3), as replaced by Law 4280/2014, art. 36), a permission the 2026 Framework (Section 6.4) restates for forests and reforestable land (Ministry of Environment and Energy, 2026, art. 5(D)). The Council of State in plenary, applying arts. 45 and 58 as they then stood, held those provisions compatible with the Constitution provided that each approval is specifically reasoned and shows the work on that land to be absolutely necessary and pressing for a purpose of particular social, national or economic importance (Council of State, 2012). Legal commentators read the decision in opposite ways, as removing any incentive to burn (Menoudakos, 2021) or as hollowing out the constitutional protection (Pavlaki, 2024). Burnt status therefore does not categorically bar wind siting under Greek law, nor is it required for it. We take no position in that debate; our results concern only whether the fleet's siting pattern shows the signature the claim implies. Where our approach adds value is methodological, in showing that a base-rate denominator, a time-ordered test, and attention to the physical versus administrative unit are what a defensible answer requires, and that a naive base-rate analysis can otherwise leave a licence-level association that no physical grouping of the same turbines reproduces.

6.4 Limitations

Several limitations qualify the findings. The time-ordered test rests on a record linkage rather than a registry key. Installation-licence dates were matched to stations on company and site tokens in free-text administrative acts, which resolved 245 of the 437 stations and 87 to 219 usable events depending on specification. Acts that omit either the company name or the site cannot be matched, so the unmatched stations are not missing at random and the temporal result speaks to the matched subset rather than to the whole fleet.

Three further limitations concern the definition of the available set. First, the eligible universe is defined by physical suitability alone, whereas Greek siting is also constrained by the spatial planning framework for renewable energy, statutory exclusion zones, protection regimes and grid access; the land that is realistically permittable is therefore narrower than the land we treat as available. Regulatory exclusions are themselves spatially structured, so this omission could bias measured preference in either direction, depending on whether the land it removes is more or less fire-prone than the land it leaves in; the direction and size are not estimated here. The framework in force throughout the fire record was the 2008 special framework for renewable energy (the 2008 Framework; Coordination Committee on Spatial Planning and Sustainable Development, 2008); production licences issued before its publication in December 2008, 277 of the 412 dated licences, were sited under the regime that preceded it. Its successor, approved in August 2026 (the 2026 Framework; Ministry of Environment and Energy, 2026), repeals the 2008 Framework and widens the exclusion zones for wind installations, among them Special Protection Areas, land above 1,200 m, small islands and the Athens and Thessaloniki metropolitan areas; it is not retroactive, since projects already operating, licensed or environmentally approved before its entry into force continue under the previous provisions, so no station analysed here was sited under it. Second, the thresholds defining the universe are calibrated to the existing fleet, which makes the available set resemble occupied land and can likewise attenuate estimated preference toward the null; the threshold grid probes this but cannot remove it. Third, the universe is defined once and held fixed, whereas eligibility evolved over 2010 to 2024 as technology, protection and grid access changed, so the risk set in the survival model is more static than the real landscape.

CORINE is a single 2018 snapshot, and for fires occurring before 2018 it already reflects post-fire land cover, so the fuel covariate carries measurement error and probably under-adjusts; the true landscape-explained component could be larger than estimated here, potentially reducing the residual. The MODIS-based EFFIS product maps only fires above about 30 ha, so small fires are absent. This matters for the specific mechanism alleged: a fire lit to clear a single development site need not grow into a mapped perimeter, so the perimeter-based tests speak most strongly to larger fires and could miss small, targeted burns entirely. The ignition analysis mitigates this only partly, because active-fire detections are anchored to mapped perimeters; a sensitivity using FIRMS detections not associated with any mapped perimeter would address it more directly and is left for future work.

Commissioning dates for bracketed stations use interval midpoints, and the incident-event set for Test C is small, between 87 and 219 depending on specification, so the time-ordered test rests on few events; it is the commissioning-

based sensitivity, not the licence-based test, that gives specification-dependent results. Dating the event at commissioning also censors structurally: with fire-to-installation gaps of six to seven years at the median and up to twelve (Table 9), fires from the later years of the window cannot yield an observed commissioning event before the 2024 cutoff, which is a further reason the installation licence is the primary event. No choice of event escapes the start of the fire record in 2010, and it is that start, rather than the event definition, that is the binding limitation on the temporal test: because most siting decisions were taken before 2010 (Section 4.4), including those behind most Test C events (78 of the 124 grant-basis events, 63%, and 136 of the 219 in the wider set, 62%, belong to stations whose production licence predates 2010), the time-ordered test asks whether a prior fire hastened the installation-licence step for projects whose location was largely already fixed, not whether fire preceded the choice of site. Test B counts any within-window overlap, including post-installation fires, which is appropriate for a spatial-association question but not for a temporal one, and is the reason the temporal question is handled separately by Test C.

A limitation concerns fire origin versus extent. Our primary exposure is the extent of each burnt area, where a fire eventually reached, not where it was ignited, so a turbine can count as near a fire that spread to it from a distant origin, even though the claim concerns where fires are started. We addressed this with satellite active-fire detections, taking the earliest detection within 1 km of each perimeter as its ignition point, and the result was null at every unit (Section 5.3). Two caveats remain: a satellite detection is a located hotspot with positioning error of a few hundred metres to about a kilometre, not a surveyed point of origin, and an ignition hotspot was recoverable for 97% of perimeters, leaving a small fraction of mostly small or brief fires unrepresented. The most direct test would use cause-attributed ground ignition records, such as the fire-service point data available from 2020 onward.

The analysis also addresses only whether siting is associated with burnt land; it does not assess the net effect of wind development on fire regimes, positive or negative, such as the role of access roads in suppression or of construction activity in ignition risk, which lies beyond its scope. Nor do the results say anything about fires started by wind-farm infrastructure itself, such as the overhead lines that connect a farm to the grid; that is a question about construction and operation rather than siting, and it is not examined here. Finally, the analysis speaks to the systematic pattern across the fleet, not to any individual project, which it can neither implicate nor exonerate.

6.5 The modifiable areal unit problem

Beyond the Greek case, the study is a concrete instance of the modifiable areal unit problem in infrastructure siting (Fotheringham & Wong, 1991; Jelinski & Wu, 1996; Openshaw, 1984). Whether a set of locations lies preferentially on land of a given type depends jointly on the unit of analysis, the scale at which exposure is measured and the completeness of the landscape controls, and an association can be present at an administrative unit and absent at a physical one without either being wrong, because the two units answer different questions. The unit should therefore be chosen and justified against the question being asked, and where the answer depends on that choice, both units should be reported. The base-rate and time-ordered framework used here is portable to other contested siting claims, in fire-prone regions and elsewhere.

7. Conclusions

Across temporal-precedence, spatial case-control, and time-ordered survival tests, evaluated from the point to 5 km and interrogated for landscape confounding, unit definition, and time gaps, the national fleet does not display the spatial or temporal pattern expected under a systematic burn-to-build mechanism. A landscape-scale association appears only when administrative licences are counted as independent units; it is absent at the turbine scale and at every physical grouping of turbines, and reflects the unit of analysis as much as any geographic preference, a dependence we treat as an instance of the modifiable areal unit problem. We read the residual association as shared occupancy of dry, exposed uplands by wind resource and fire rather than as siting on burnt land, an interpretation consistent with the covariate structure rather than a directly tested result. Replacing fire extent with estimated ignition points leaves the spatial and time-ordered tests without a significant association, within the positional limits of satellite detections, and so supports the conclusion; a still more direct test would use cause-attributed ground ignition records.

Intent is not observable from siting and fire data, and this population-level finding neither establishes nor excludes that any individual project was sited on burnt land. The perimeter-based tests concern mapped fires above about 30 ha, so a fire small enough to clear one development site without growing into a mapped perimeter lies outside the

https://doi.org/10.48088/ejg.s.str.17.1.399.424

reach of this evidence. The null time ordering gives no support to a burn-to-build mechanism, and the long fire-to-installation gaps are consistent with that, although gaps are long partly by construction: most siting predates the 2010 start of the record, the gaps run to commissioning rather than to siting, and small fires are omitted. One result runs the other way and we do not set it aside: the number of farms with a catchment fire in the three years after the production licence exceeds the number expected from local fire rates at every catchment, by 44 to 73%, although the excess is not significant at any of them and the smallest one-sided tail probability is 0.058. It is too weak to carry an inference and too consistent across catchments to ignore, and it is the result most worth revisiting on longer records.

The main lessons are methodological and transferable: the answer to a contested siting claim depends on the base rate, the catchment scale, the completeness of landscape controls, and, as this case shows sharply, on whether the unit of analysis is physical or administrative.

Funding: This research received no external funding.

Conflicts of Interest: The author is an independent researcher with no financial or professional ties to the wind-energy industry, no funding from energy companies or industry associations, and no role in wind-farm development, licensing, or opposition.

Software and Reproducibility: Analyses were implemented in Python using geopandas and rasterio for geospatial processing, statsmodels for the logistic models (Seabold & Perktold, 2010), lifelines for the time-varying Cox model (Davidson-Pilon, 2019), and scikit-learn for the permutation inference. All derived datasets and the full analysis code are openly archived (see Data availability).

Data Availability Statement: The derived datasets, including the merged fire perimeters, the eligible-universe raster, the terrain and land-cover layers, and the case-control and per-farm tables, together with the full analysis code and the verification suite, are archived at Zenodo (https://doi.org/10.5281/zenodo.21261872). Input products are third-party and used under their own licences: the RAAEY registry, OpenStreetMap, Copernicus EFFIS, the Global Wind Atlas, the Copernicus GLO-90 digital elevation model, CORINE, Natura 2000, and NASA FIRMS active-fire detections.

Acknowledgements: The author acknowledges the use of an AI assistant to support the research process, specifically the drafting and debugging of analysis code, language editing of the manuscript, and preparation of figures; the study design, statistical specifications, verification of results, and interpretation are the author's own, and the author is solely accountable for the work. The providers of the open datasets used, including Copernicus EFFIS, the European Environment Agency, the Global Wind Atlas, and NASA FIRMS (LANCE), are gratefully acknowledged.

Appendix

Supporting tables cited in the Methods, Results and Discussion. Table A1 reports the full covariate structure of the licence-unit Test B specification discussed in Section 6.2; Table A2 reports the sensitivity of the licence-unit residual to the definition of fire-prone fuel discussed in Section 5.2; Table A3 lists the control-draw convention behind each table (Section 4.5).

Table A1. Full model coefficients for the licence-unit Test B specification at 2 km with the fuel covariate. Continuous covariates are standardised, so odds ratios are per standard deviation. As in Table 3, estimates are means over 20 independent control draws (seeds 1 to 20); intervals combine within-draw and between-draw variance.

Term	Odds ratio	95% CI	p
Burnt within 2 km	1.34	1.04–1.72	0.024
Wind speed	1.92	1.78–2.08	<0.001
Slope	0.65	0.56–0.74	<0.001
Elevation	1.09	0.94–1.27	0.242
Northness	1.07	0.95–1.20	0.276
Eastness	0.93	0.82–1.05	0.237
Natura 2000	0.39	0.30–0.53	<0.001

Term	Odds ratio	95% CI	p
Fuel (fire-prone fraction)	2.61	2.12–3.22	<0.001

Source: author's analysis.

Table A2. Sensitivity of the licence-unit 2 km fuel-adjusted burnt odds ratio to the definition of fire-prone fuel. The definition used here uses CORINE classes 311, 312, 313, 321, 322, 323, 324 and 333; the narrow woody definition drops natural grassland (321) and sparsely vegetated areas (333); the agriculture-inclusive definition adds the arable, permanent-crop, pasture and heterogeneous agricultural classes (211 to 213, 221 to 223, 231, 241 to 244); and the EFFIS and FirEUrisk aligned definition adds only the two mixed agriculture and natural vegetation classes (243, 244). All estimates in this table use the single fixed control draw; see Section 4.5.

Fire-prone definition	Share of universe	Odds ratio	95% CI	p
Definition used here (8 CORINE classes)	53.8%	1.40	1.09–1.80	0.008
Woody narrow (forest and shrub only)	38.6%	1.54	1.20–1.97	0.001
Agriculture-inclusive	86.3%	1.50	1.17–1.93	0.002
EFFIS/FirEUrisk-aligned	62.2%	1.34	1.04–1.72	0.022

Source: author's analysis. Definitions follow the EFFIS European Fuel Map (López et al., 2002) and the FirEUrisk classification (Aragoneses et al., 2023).

Table A3. Control-draw convention used by each table. Single-draw tables share one fixed sample of 30,000 control points; multi-draw tables average twenty independent samples and combine within-draw and between-draw variance. Figures from the two conventions are never compared with each other in the text.

Table	Quantity	Control-draw convention
3	Test B odds ratios by unit and scale	mean over 20 draws (seeds 1 to 20), Rubin's rule
4 and 5	wind-by-slope threshold grid	single draw (seed 42)
6	physical-cluster and licence units	single draw (seed 42)
7	ignition-point exposure	single draw (seed 42)
8	Test C hazard ratios	single draw (seed 42) of 30,000 controls
A1	full model coefficients	mean over 20 draws, Rubin's rule
A2	fuel-definition sensitivity	single draw (seed 42)

https://doi.org/10.48088/ejg.s.str.17.1.399.424

Table	Quantity	Control-draw convention
Figure 4	Test B odds ratios across catchment radius	mean over 20 draws (seeds 1 to 20), Rubin's rule, from outputs/seed_sweep.csv
Section 5.2 text	representative-point comparison (hull centroid, mean coordinate, turbine nearest the centroid, random turbine)	mean over the same 20 draws
Section 5.2 text	permutation test on the 2 km fuel-adjusted licence estimate	1,000 label permutations under each of six independent draws; range and median p reported
Primary cell under both	licence unit, 2 km, fuel-adjusted, hull centroid	1.40 (single draw) against 1.34 (20 draws); mean-coordinate centroid 1.41 against 1.35

Source: author's analysis.

References

Aragoneses, E., García, M., Salis, M., Ribeiro, L. M., & Chuvieco, E. (2023). Classification and mapping of European fuels using a hierarchical, multipurpose fuel classification system. *Earth System Science Data, 15*(3), 1287–1315. https://doi.org/10.5194/essd-15-1287-2023

Boyce, M. S., Vernier, P. R., Nielsen, S. E., & Schmiegelow, F. K. A. (2002). Evaluating resource selection functions. *Ecological Modelling, 157*(2–3), 281–300. https://doi.org/10.1016/S0304-3800(02)00200-4

Coordination Committee on Spatial Planning and Sustainable Development. (2008). Decision 49828/12.11.2008, *Έγκριση ειδικού πλαισίου χωροταξικού σχεδιασμού και αειφόρου ανάπτυξης για τις ανανεώσιμες πηγές ενέργειας και της στρατηγικής μελέτης περιβαλλοντικών επιπτώσεων αυτού* [Approval of the special framework for spatial planning and sustainable development for renewable energy sources and of its strategic environmental assessment]. ΦΕΚ Β΄ 2464/3.12.2008.

Council of State (Plenary). (2012). *Decision 2499/2012* [Development of a wind power station within reforestable land] (Greece). https://nomosphysis.org.gr/14813/ste-ol-24992012-anaptyksi-aspie-entos-anadasoteon-ektaseon/

Cox, D. R. (1972). Regression models and life-tables. *Journal of the Royal Statistical Society: Series B, 34*(2), 187–220. https://doi.org/10.1111/j.2517-6161.1972.tb00899.x

Davidson-Pilon, C. (2019). lifelines: Survival analysis in Python. *Journal of Open Source Software, 4*(40), 1317. https://doi.org/10.21105/joss.01317

Denholm, P., Hand, M., Jackson, M., & Ong, S. (2009). *Land-use requirements of modern wind power plants in the United States* (NREL/TP-6A2-45834). National Renewable Energy Laboratory. https://doi.org/10.2172/964608

Devine-Wright, P. (2009). Rethinking NIMBYism: The role of place attachment and place identity in explaining place-protective action. *Journal of Community & Applied Social Psychology, 19*(6), 426–441. https://doi.org/10.1002/casp.1004

Diffendorfer, J. E., & Compton, R. W. (2014). Land cover and topography affect the land transformation caused by wind facilities. *PLoS ONE, 9*(2), e88914. https://doi.org/10.1371/journal.pone.0088914

Efstathiou, N. (2025). *Extinguishing wildfire misinformation: Case-studies & avenues for improvement* [Journalist fellowship paper]. Reuters Institute for the Study of Journalism, University of Oxford. https://reutersinstitute.politics.ox.ac.uk/sites/default/files/2025-11/RISJPaper_NikoE_TT25_Final2.pdf

Elliott, P., & Wartenberg, D. (2004). Spatial epidemiology: Current approaches and future challenges. *Environmental Health Perspectives, 112*(9), 998–1006. https://doi.org/10.1289/ehp.6735

European Environment Agency. (2019a). *CORINE Land Cover 2018* [Data set]. https://land.copernicus.eu/en/products/corine-land-cover

European Environment Agency. (2019b). *Natura 2000 data: The European network of protected sites* [Data set]. https://www.eea.europa.eu/data-and-maps/data/natura-11

European Forest Fire Information System. (2024). *Burnt areas* [Data set]. Copernicus Emergency Management Service. https://forest-fire.emergency.copernicus.eu

European Space Agency, & Airbus. (2022). *Copernicus GLO-90 Digital Elevation Model* [Data set]. https://spacedata.copernicus.eu

Fotheringham, A. S., & Wong, D. W. S. (1991). The modifiable areal unit problem in multivariate statistical analysis. *Environment and Planning A, 23*(7), 1025–1044. https://doi.org/10.1068/a231025

Ganteaume, A., Camia, A., Jappiot, M., San-Miguel-Ayanz, J., Long-Fournel, M., & Lampin, C. (2013). A review of the main driving factors of forest fire ignition over Europe. *Environmental Management, 51*(3), 651–662. https://doi.org/10.1007/s00267-012-9961-z

Global Wind Atlas. (2023). *Mean wind speed at 100 m* [Data set]. Technical University of Denmark (DTU Wind Energy). https://globalwindatlas.info

Harrison-Atlas, D., Lopez, A., & Lantz, E. (2022). Dynamic land use implications of rapidly expanding and evolving wind power deployment. *Environmental Research Letters, 17*(4), 044064. https://doi.org/10.1088/1748-9326/ac5f2c

Hellenic Fire Service. (2024). *Statistical data on forest fires* [Data set]. https://www.fireservice.gr/el_GR/synola-dedomenon

Hellenic Parliament. (2019). *Σύνταγμα της Ελλάδος* [The Constitution of Greece], as revised by the Resolution of 25 November 2019. ΦΕΚ Α΄ 211/24.12.2019.

Hellenic Wind Energy Association. (2025). *Wind turbines and forest fires in Greece: A quantitative analysis* (July 2025 update). https://eletaen.gr/wp-content/uploads/2025/09/2025-09-09-WTs-and-Fires-in-Greece_Eletaen-Quantitative-Analysis_July2025.pdf

Jelinski, D. E., & Wu, J. (1996). The modifiable areal unit problem and implications for landscape ecology. *Landscape Ecology, 11*(3), 129–140. https://doi.org/10.1007/BF02447512

Johnson, C. J., Nielsen, S. E., Merrill, E. H., McDonald, T. L., & Boyce, M. S. (2006). Resource selection functions based on use-availability data: Theoretical motivation and evaluation methods. *The Journal of Wildlife Management, 70*(2), 347–357. https://doi.org/10.2193/0022-541X(2006)70[347:RSFBOU]2.0.CO;2

Johnson, D. H. (1980). The comparison of usage and availability measurements for evaluating resource preference. *Ecology, 61*(1), 65–71. https://doi.org/10.2307/1937156

Kati, V. I., Kassara, C., Panagos, P., Tampouratzi, L., Gotsis, D., Tzortzakaki, O., Petridou, M., Psaralexi, M., Sidiropoulos, L., Vasilakis, D., Zakkak, S., Galani, A., & Mpoukas, N. (2023). The overlooked threat of land take from wind energy infrastructures: Quantification, drivers and policy gaps. *Journal of Environmental Management, 348*, 119340. https://doi.org/10.1016/j.jenvman.2023.119340

Koutsias, N., Xanthopoulos, G., Founda, D., Xystrakis, F., Nioti, F., Pleniou, M., Mallinis, G., & Arianoutsou, M. (2013). On the relationships between forest fires and weather conditions in Greece from long-term national observations (1894–2010). *International Journal of Wildland Fire, 22*(4), 493–507. https://doi.org/10.1071/WF12003

Law 998/1979, *Περί προστασίας των δασών και των δασικών εν γένει εκτάσεων της Χώρας* [On the protection of forests and forest lands of the country], ΦΕΚ Α΄ 289/29.12.1979, as amended, inter alia by Law 4280/2014, art. 36 (arts. 45 to 61), ΦΕΚ Α΄ 159/8.8.2014 (Greece).

López, A. S., San-Miguel-Ayanz, J., & Burgan, R. E. (2002). Integration of satellite sensor data, fuel type maps and meteorological observations for evaluation of forest fire risk at the pan-European scale. *International Journal of Remote Sensing, 23*(13), 2713–2719. https://doi.org/10.1080/01431160110107761

Manly, B. F. J., McDonald, L. L., Thomas, D. L., McDonald, T. L., & Erickson, W. P. (2002). *Resource selection by animals: Statistical design and analysis for field studies* (2nd ed.). Kluwer Academic Publishers. https://doi.org/10.1007/0-306-48151-0

Manousos, G. (2024, July 12). *Αμέτρητες άδειες αιολικών πάρκων σε καμένες εκτάσεις γης* [Countless wind-farm licences on burnt land] [Parliamentary question to the Minister of Environment and Energy]. Hellenic Parliament. https://www.hellenicparliament.gr/UserFiles/c0d5184d-7550-4265-8e0b-078e1bc7375a/12633435.pdf

Menoudakos, K. (2021, August 24). *Το ΣτΕ, οι ανεμογεννήτριες και οι αναδασωτέες εκτάσεις* [The Council of State, wind turbines and reforestable land]. Nomos + Physis. https://nomosphysis.org.gr/21459/to-ste-oi-anemogennitries-kai-oi-anadasotees-ektaseis/

Metron Analysis. (2022). *Πανελλαδική έρευνα για την κλιματική αλλαγή: Αντιλήψεις, απειλές και προκλήσεις για μια νέα περιβαλλοντική κουλτούρα* [Nationwide survey on climate change: Perceptions, threats and challenges for a new environmental culture] [Survey report for the Ministry of Climate Crisis and Civil Protection]. diaNEOsis. https://www.dianeosis.org/wp-content/uploads/2022/06/climatechange_survey.pdf

Ministry of Environment and Energy. (2026). Decision ΥΠΕΝ/ΔΝΕΠ/89998/3072, *Έγκριση Ειδικού Χωροταξικού Πλαισίου για τις Ανανεώσιμες Πηγές Ενέργειας (ΑΠΕ) και περιβαλλοντική έγκριση αυτού* [Approval of the Special Spatial Framework for Renewable Energy Sources and its environmental approval]. ΦΕΚ Δ΄ 694/19.08.2026.

Moreira, F., Viedma, O., Arianoutsou, M., Curt, T., Koutsias, N., Rigolot, E., Barbati, A., Corona, P., Vaz, P., Xanthopoulos, G., Mouillot, F., & Bilgili, E. (2011). Landscape–wildfire interactions in southern Europe: Implications for landscape management. *Journal of Environmental Management, 92*(10), 2389–2402. https://doi.org/10.1016/j.jenvman.2011.06.028

NASA FIRMS. (2024). *Active fire data: MODIS and VIIRS detections* [Data set]. NASA Land, Atmosphere Near real-time Capability for EOS (LANCE). https://firms.modaps.eosdis.nasa.gov

Northrup, J. M., Hooten, M. B., Anderson, C. R., Jr., & Wittemyer, G. (2013). Practical guidance on characterizing availability in resource selection functions under a use-availability design. *Ecology, 94*(7), 1456–1463. https://doi.org/10.1890/12-1688.1

Openshaw, S. (1984). *The modifiable areal unit problem* (Concepts and Techniques in Modern Geography No. 38). Geo Books.

OpenStreetMap. (2024). *Wind turbine data for Greece* [Data set]. https://www.openstreetmap.org

Palaiologou, P., Kalabokidis, K., Troumbis, A., Day, M. A., Nielsen-Pincus, M., & Ager, A. A. (2021). Socio-ecological perceptions of wildfire management and effects in Greece. *Fire, 4*(2), 18. https://doi.org/10.3390/fire4020018

Panizio, E., & Canetta, T. (2024, January 25). *Wind turbines and poisoned animals: A "New Denial"'s popular disinformation narrative against renewable energy*. European Digital Media Observatory. https://edmo.eu/publications/wind-turbines-and-poisoned-animals-a-new-denials-popular-disinformation-narrative-against-renewable-energy/

Pausas, J. G., & Fernández-Muñoz, S. (2012). Fire regime changes in the Western Mediterranean Basin: From fuel-limited to drought-driven fire regime. *Climatic Change, 110*(1–2), 215–226. https://doi.org/10.1007/s10584-011-0060-6

Pavlaki, S. E. (2024, September 1). *Νομικά ζητήματα από την εγκατάσταση αιολικών σταθμών σε αναδασωτέες εκτάσεις* [Legal issues arising from the installation of wind farms on reforestable land]. dasarxeio.com. https://dasarxeio.com/2024/09/01/139178/

Pedregosa, F., Varoquaux, G., Gramfort, A., Michel, V., Thirion, B., Grisel, O., Blondel, M., Prettenhofer, P., Weiss, R., Dubourg, V., Vanderplas, J., Passos, A., Cournapeau, D., Brucher, M., Perrot, M., & Duchesnay, É. (2011). Scikit-learn: Machine learning in Python. *Journal of Machine Learning Research, 12*, 2825–2830. https://jmlr.org/papers/v12/pedregosa11a.html

Rand, J., & Hoen, B. (2017). Thirty years of North American wind energy acceptance research: What have we learned? *Energy Research & Social Science, 29*, 135–148. https://doi.org/10.1016/j.erss.2017.05.019

Regulatory Authority for Waste, Energy and Water. (2024). *Register of electricity production licences* [Data set]. https://www.raaey.gr

San-Miguel-Ayanz, J., Durrant, T., Boca, R., Maianti, P., Libertà, G., Jacome Felix Oom, D., Branco, A., De Rigo, D., Suarez-Moreno, M., Ferrari, D., Roglia, E., Scionti, N., Broglia, M., Onida, M., Tistan, A., & Loffler, P. (2024). *Forest fires in Europe, Middle East and North Africa 2023* (JRC139704, EUR 40092). Publications Office of the European Union. https://doi.org/10.2760/8027062

San-Miguel-Ayanz, J., Moreno, J. M., & Camia, A. (2013). Analysis of large fires in European Mediterranean landscapes: Lessons learned and perspectives. *Forest Ecology and Management, 294*, 11–22. https://doi.org/10.1016/j.foreco.2012.10.050

Seabold, S., & Perktold, J. (2010). statsmodels: Econometric and statistical modeling with Python. *Proceedings of the 9th Python in Science Conference*, 92–96. https://doi.org/10.25080/Majora-92bf1922-011

Vlamakis, A., Eleftheriou, I., & Dima, S. (2025). *The real and unreal correlation between wind turbines and wildfires: Lessons from Greece* [Conference poster P122]. 8th Conference on Wind Energy and Wildlife Impacts (CWW 2025), Montpellier, France, 8–12 September 2025.

Vlamakis, A., Eleftheriou, I., Dima, S., Karra, E., & Papastamatiou, P. (2026). Beyond the footprint: Empirical land use and environmental patterns of wind energy in mountainous landscapes. *Land, 15*(2), 344. https://doi.org/10.3390/land15020344

Winter, K., Hornsey, M. J., Pummerer, L., & Sassenberg, K. (2022). Anticipating and defusing the role of conspiracy beliefs in shaping opposition to wind farms. *Nature Energy, 7*(12), 1200–1207. https://doi.org/10.1038/s41560-022-01164-w

Winter, K., Hornsey, M. J., Pummerer, L., & Sassenberg, K. (2024). Public agreement with misinformation about wind farms. *Nature Communications, 15*, 8888. https://doi.org/10.1038/s41467-024-53278-2

Wüstenhagen, R., Wolsink, M., & Bürer, M. J. (2007). Social acceptance of renewable energy innovation: An introduction to the concept. *Energy Policy, 35*(5), 2683–2691. https://doi.org/10.1016/j.enpol.2006.12.001

Disclaimer/Publisher's Note: The statements, opinions and data contained in all publications are solely those of the individual author(s) and contributor(s) and not of EUROGEO and/or the editor(s). EUROGEO and/or the editor(s) disclaim responsibility for any injury to people or property resulting from any ideas, methods, instructions, or products referred to in the content.

European Journal of Geography